

Bacterial cupredoxin azurin as an inducer of apoptosis and regression in human breast cancer

Vasu Punj^{1,2}, Suchita Bhattacharyya², Djenann Saint-Dic¹, Chenthamarakshan Vasu³, Elizabeth A Cunningham¹, Jewell Graves¹, Tohru Yamada², Andreas I Constantinou¹, Konstantin Christov¹, Bethany White¹, Gang Li⁴, Dibyen Majumdar⁴, Ananda M Chakrabarty² and Tapas K Das Gupta^{*1}

¹Department of Surgical Oncology, University of Illinois at Chicago, 840 South Wood Street, M/C 820, Chicago, IL 60612, USA;

²Department of Microbiology and Immunology, University of Illinois at Chicago, 901 S. Wolcott Ave., M/C 790, Chicago, IL 60612-7344, USA;

³Department of Surgery, University of Illinois at Chicago, 840 S. Wood St., M/C 958, Chicago, IL 60612, USA;

⁴Department of Mathematics, Statistics, and Computer Sciences, 851 S. Morgan, MC 249, University of Illinois at Chicago, Chicago, IL 60607, USA

Azurin, a copper-containing redox protein released by the pathogenic bacterium *Pseudomonas aeruginosa*, is highly cytotoxic to the human breast cancer cell line MCF-7, but is less cytotoxic toward p53-negative (MDA-MB-157) or nonfunctional p53 cell lines like MDD2 and MDA-MB-231. The purpose of this study was to investigate the underlying mechanism of the action of bacterial cupredoxin azurin in the regression of breast cancer and its potential chemotherapeutic efficacy. Azurin enters into the cytosol of MCF-7 cells and travels to the nucleus, enhancing the intracellular levels of p53 and Bax, thereby triggering the release of mitochondrial cytochrome *c* into the cytosol. This process activates the caspase cascade (including caspase-9 and caspase-7), thereby initiating the apoptotic process. Our results indicate that azurin-induced cell death stimuli are amplified in the presence of p53. *In vivo* injection of azurin in immunodeficient mice harboring xenografted human breast cancer cells in the mammary fat pad leads to statistically significant regression (85%, $P = 0.0179$, Kruskal–Wallis Test) of the tumor. In conclusion, azurin blocks breast cancer cell proliferation and induces apoptosis through the mitochondrial pathway both *in vitro* and *in vivo*, thereby suggesting a potential chemotherapeutic application of this bacterial cupredoxin for the treatment of breast cancer.

Oncogene (2004) 23, 2367–2378. doi:10.1038/sj.onc.1207376

Published online 23 February 2004

Keywords: cupredoxin azurin; breast cancer; apoptosis

Introduction

With one million new cases in the world each year, breast cancer is the most common malignancy in women

and constitutes 18% of all female cancers (Jemal *et al.*, 2002). Although there has been a slight decrease in mortality in breast cancer patients (Schiffman *et al.*, 2002), it is not uncommon for even early-stage breast cancer to metastasize. Therefore, novel therapeutic strategies are constantly being pursued (Bange *et al.*, 2001). Various candidates for breast cancer therapy include differentiating agents, angiogenesis inhibitors, vaccines, monoclonal antibodies, and approaches using dendritic cells (Tangri *et al.*, 2001). Recently, interest was rekindled in the old idea (Coley, 1911) of using live or attenuated pathogenic bacteria or their products in the treatment of cancer (Lamoureux *et al.*, 1976; da Rocha *et al.*, 2001; Chakrabarty, 2003; Sinha, 2003).

The infection of tumor-bearing mice with live attenuated cells of *Salmonella typhimurium* has been reported to produce tumor regression (Pawelek *et al.*, 1997). A significant regression of subcutaneous tumors in mice was observed by combining anaerobic bacteria with various chemotherapeutic agents (Dang *et al.*, 2001). The antitumor activity of these pathogens has been attributed to the activation of an immune response against tumor antigens (Paglia and Guzman, 1998), to the preferential growth of certain bacteria within the tumor (Sznol *et al.*, 2000), or to the inhibition of angiogenesis (Hunter *et al.*, 2001). However, live microorganisms with or without chemotherapeutic agents produce significant morbidity and mortality (Alexandroff *et al.*, 1999; Dang *et al.*, 2001). Hence, studies are in progress to identify pure metabolites of microbial origin or any other components of the microbial cell that might have antitumor activity. One such example is the identification of secondary metabolites, epothilones A and B of the myxobacterium *Sorangium cellulosum*, which have shown both *in vitro* and *in vivo* cytotoxicity in various cancer cells, including MCF-7 cells (Chou *et al.*, 1998; Altmann *et al.*, 2000).

We recently reported that azurin, a cupredoxin type of electron transfer agent elaborated by the bacterium *Pseudomonas aeruginosa*, triggers cell death in well-

*Correspondence: TK Das Gupta; E-mail: tkdg@uic.edu

Received 23 May 2003; revised 5 November 2003; accepted 19 November 2003

established J774 macrophages—a transformed cell line from murine reticulum cell sarcoma (Ralph and Nakoinz, 1975). *In vitro* studies revealed a direct physical interaction between azurin and p53 (Punj *et al.*, 2003). After internalization within J774 cells, azurin forms a complex with the tumor suppressor protein p53, stabilizes it, and enhances its intracellular level, thereby inducing apoptosis via caspase-mediated mitochondrial pathways (Yamada *et al.*, 2002a).

The role of azurin as a potent inducer of apoptosis in transformed macrophages prompted us to examine if azurin might have such an effect in human cancer cells. We have observed that azurin could trigger cell death in some cancer cells, such as melanoma (Yamada *et al.*, 2002b). Apoptosis is an essential process in cellular development and in maintaining cellular homeostasis; the failure of damaged cells to undergo apoptosis contributes to cancer progression by allowing the DNA-damaged cells to persist. In the mitochondrial apoptotic pathway, its activation depends on mitochondrial membrane disruption and the release of cytochrome *c*. Once activated, caspase-9 and caspase-7/3 have been shown to act on mitochondria to further disrupt their integrity, thus creating a self-amplifying feedback loop (Chandler *et al.*, 1998; Tong *et al.*, 2002). However, MCF-7 human breast cancer cells lack caspase-3, a crucial component of apoptosis, but they remain responsive to many apoptotic stimuli (Le *et al.*, 2001; Liang *et al.*, 2001; Cuvillier *et al.*, 2001; Hu *et al.*, 2002; McGee *et al.*, 2002). Therefore, in the present study, we first investigated how azurin exerts its effect on certain molecular markers of apoptosis in breast cancer cells with differing p53 statuses and then studied its effect on breast cancer growth in an athymic mouse xenograft model.

Results

Effect of azurin treatment on the growth of various breast cancer cell lines with different p53 status

The treatment of various breast cancer cell lines with 3.5–64 μM of azurin for 24 h resulted in the inhibition of cell proliferation in a dose- and time-dependent manner. The IC₅₀ dose for MCF-7 (p53 +/+) cells was 32 μM after 24 h of treatment with azurin—a dose far less than that for p53 null, MDA-MB-157 cells (53 μM) (Figure 1a). Azurin had little effect on MDD2 (containing a dominant-negative p53 variant) and MDA-MB-231 (mutant p53) cells. Approximately 29% of MCF-7 cells survived after being treated with 53 μM of azurin for 72 h (data not shown). The inhibition of cell proliferation could have been the result of apoptosis, cell cycle growth arrest, inhibition of growth, or a combination of these. We therefore next investigated whether azurin induces apoptosis in breast cancer cells.

Induction of apoptosis by azurin

In order to delineate the mechanism of action involved in azurin-induced apoptosis in breast cancer cells, a panel of breast cancer cell lines was treated with azurin

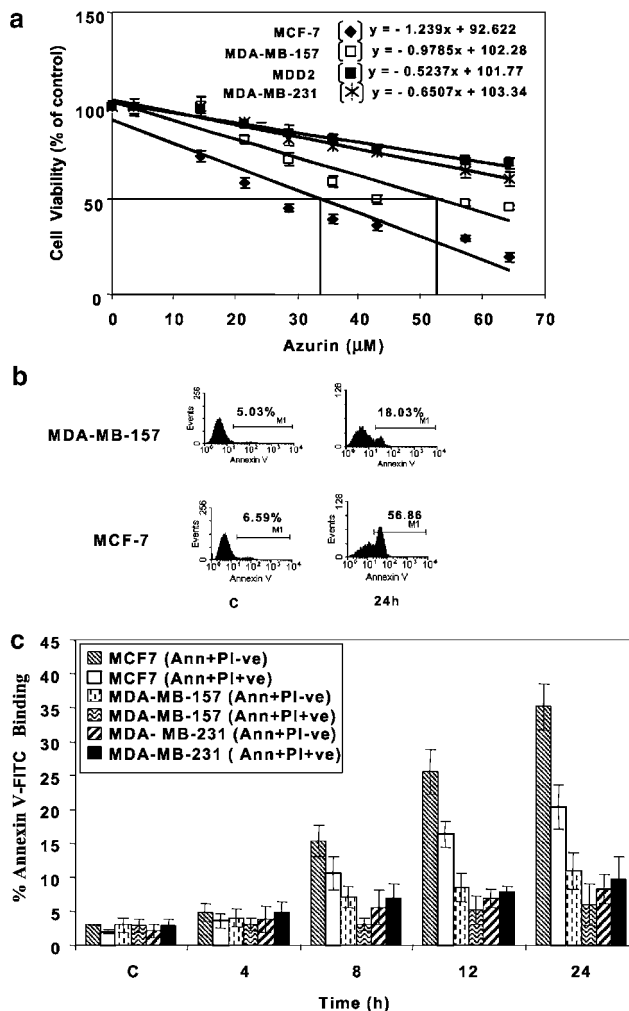


Figure 1 (a) Effect of Azurin treatment on cellular proliferation of various breast cancer cell lines. Cells were treated with various doses of azurin for 24h and cell survival was determined as described in Material and Methods. IC₅₀ represents the dose of azurin required for 50% cell death. (b) Azurin-induced time-dependent apoptosis in breast cancer cells. Cells were treated with 32 μM of azurin for various time intervals and stained with Annexin V and PI. Representative histograms of control, and 24-h time points are shown for MCF-7 and MDA-MB-157 cells. (c) Quantitative estimation of apoptosis induced in various cell lines. Cells stained with Annexin V-FITC + PI were considered as late apoptotic/necrotic cells, while cells stained with Annexin V were referred to as apoptotic cells. Data are presented as the percentage of cells in each classification. Error bars represent the mean \pm SD

and the level of apoptosis was determined with annexin V staining. The data in Figure 1b and c reveal extensive heterogeneity in the extent of apoptosis induction in the panel of cell lines. Further studies were carried out with the three representative cell lines: MCF-7 (wild-type p53), MDA-MB-157 (p53 null), and MDA-MB-231 (mutant p53). The least azurin-sensitive cell line, MDA-MB-231, displayed an increase in apoptosis of less than 15%, while the intermediately sensitive MDA-MB-157 showed an increase of 18%. MCF-7 cells exhibited a more than 50% increase in apoptosis. Analysis of the staining pattern indicated that the predominant cause of

cell death in MCF-7 was apoptosis rather than necrosis. A similar mechanism was also present in MDA-MB-157 cells, albeit to a much lesser extent (Figure 1c).

Effect of azurin on p53 expression

As azurin-induced apoptosis predominantly occurred in MCF-7 cells, we examined the effect of azurin treatment on p53 expression in the MCF-7, MDA-MB-157, and MDA-MB-231 cell lines. In MCF-7 cells treated with azurin, p53 expression reached its maximum 24 h after treatment, while it underwent no change in MDA-MB-157 cells (p53 null) and was variably downregulated in MDA-MB-231 cells (Figure 2a). We then used Western blotting to examine the subcellular distribution of p53 in the cytosol, nuclear, and mitochondrial extracts from MCF-7 cells after azurin treatment for various intervals. The level of p53 increased substantially in cytosol and nuclear extracts after 8–24 h of treatment (Figure 2b). A portion of p53 was also translocated to the mitochondria, especially after 24 h of treatment. Such translocation of p53 to the mitochondria has been shown to be specific to p53-dependent apoptosis (Marchenko *et al.*, 2000; Mihara *et al.*, 2003).

Effect of azurin treatment on the expression of pro- and antiapoptotic markers

Three cell lines (MCF-7, MDA-MB-157, and MDA-MB-231) were used to see if azurin-induced apoptosis occurs through p53-dependent modulation of *bax* and *bcl2* gene expression. In MCF-7 cells, the level of Bax gradually increased with the time of azurin treatment,

while Bcl2 levels marginally decreased. MDA-MB-157 cells showed no changes in Bax or Bcl2 levels, while MDA-MB-231 showed variable changes in both (Figure 3a). Optical density measurements were carried out to obtain quantitative values for protein expression of Bax and Bcl2. It has been shown that the ratio of Bax to Bcl2 protein expression levels dictates apoptotic cell

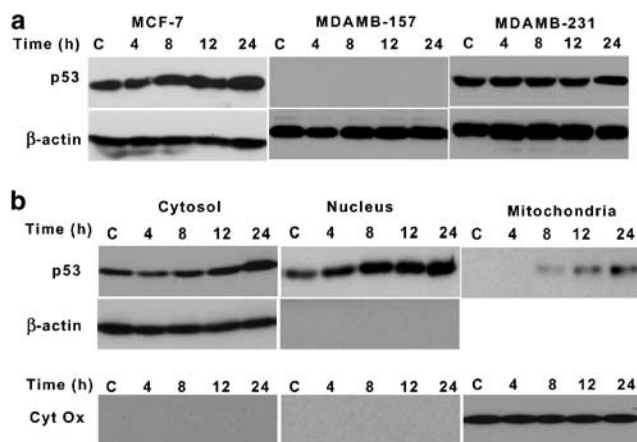


Figure 2 (a) Western blot analysis to detect p53 in cell extracts of MCF-7, MDA-MB-231, and MDA-MB-157 cells treated with azurin for the indicated time intervals. C represents control cells treated with PBS buffer. The level of p53 increased with time in MCF-7 cells, while there was a slight decrease in p53 level in MDA-MB-231 cells after 24 h of treatment. β -Actin was used as an internal loading control. (b) Subcellular distribution of p53 in MCF-7 cells treated with azurin for the indicated times. The level of p53 increased in the cytosol and nucleus with the time of treatment; a fraction of p53 is translocated to the mitochondria, especially at 12 and 24 h after treatment. β -Actin and cytochrome *c* oxidase were used as an internal control. (c) Control cells treated with PBS

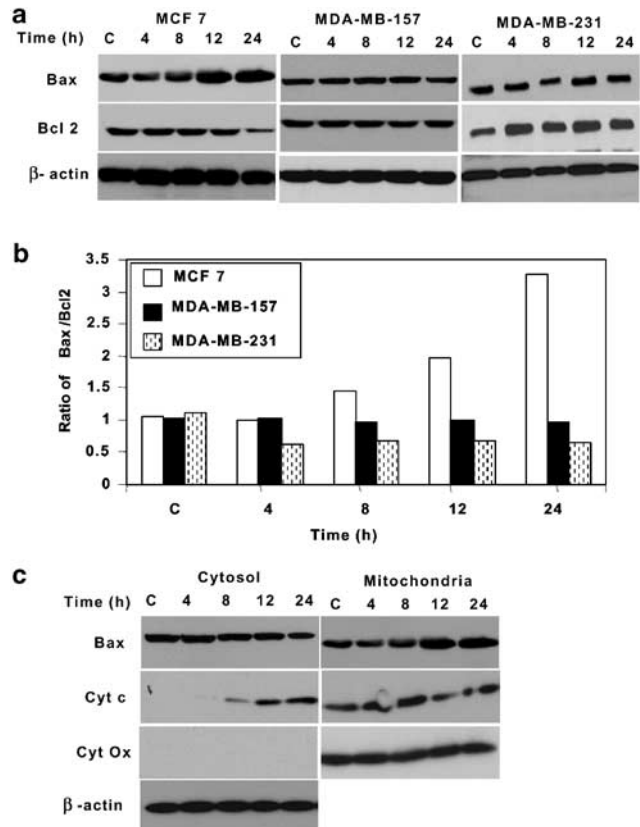


Figure 3 (a) Effect of azurin treatment on the expression of Bax and Bcl2 in MCF-7, MDA-MB-157, and MDA-MB-231 cells. The cells were treated with azurin for the indicated time and extracts were separated on SDS-PAGE and immunoblotted as described in Materials and methods. In MCF-7 cells, the level of Bax increases, while Bcl2 decreases with the time of treatment. There was no significant change in the level of either protein in MDA-MB-157 cells. In MDA-MB-231 cells, there is variation in the level of expression of Bax: it decreases at 8 h and then increases at 12 and 24 h, while the level of Bcl2 increases at 8 and 12 h but undergoes a slight decrease at 24 h. (b) Densitometric analysis of Bax and Bcl2 protein expression levels in MCF-7, MDA-MB-157, and MDA-MB-231 cells treated with azurin. Bax and Bcl2 ratio was higher only in MCF-7 cells over control. One representative graph is shown. (c) Azurin treatment induced Bax redistribution from the cytosol to the mitochondria in MCF-7 cells. After treatment with azurin for the indicated time, cytosolic and mitochondrial extracts were prepared and subjected to SDS-PAGE followed by Western blot and probed with respective antibodies. Bax level decreases after 12 and 24 h in cytosol, while its level increases in the mitochondria at the same time, indicating its accumulation in the mitochondria. This translocation occurs after the release of mitochondrial cytochrome *c* in the cytosol (8 h). (c) Azurin-induced cytochrome *c* release into the cytosol of MCF-7 cells. Cytochrome *c* in the cytosol was observed 8 h post-azurin treatment, which increased with time. Cytochrome *c* levels in mitochondria are also shown. β -Actin and cytochrome *c* oxidase were used as control for cytosol and mitochondrial fraction. *c*: control cells

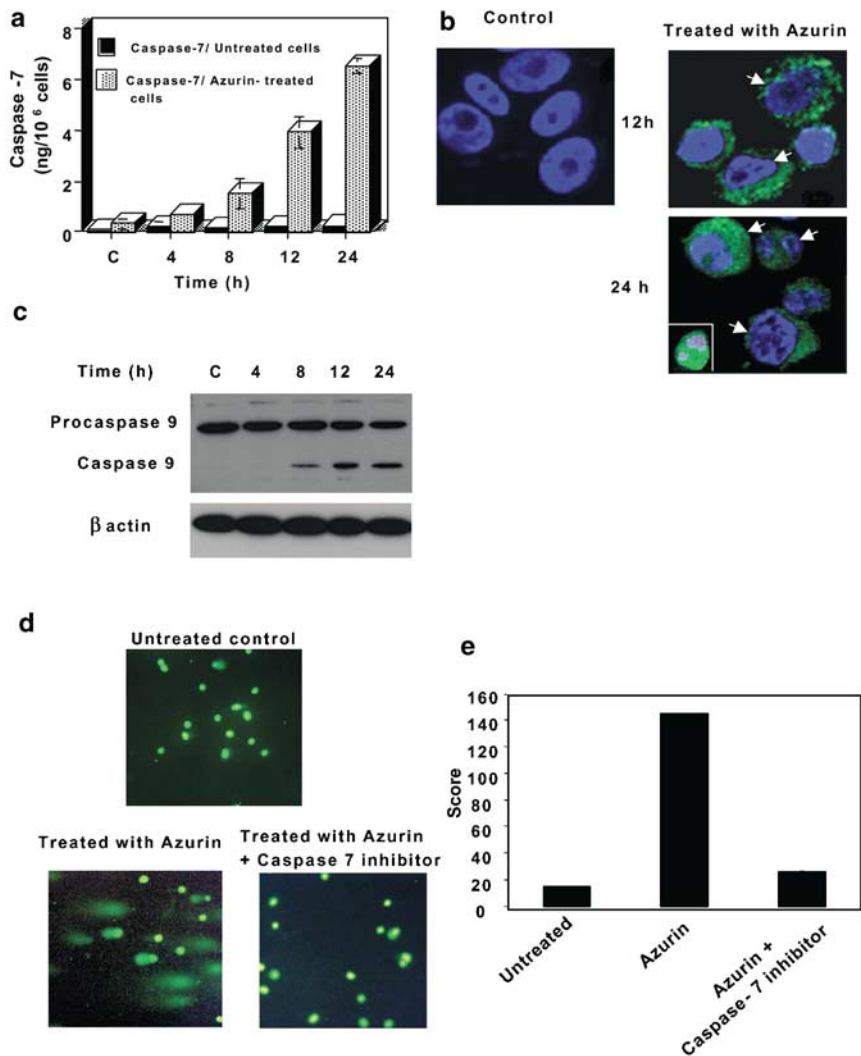


Figure 4 (a) Quantitative ELISA for the detection of cleaved caspase-7 in MCF-7 cells treated with azurin and untreated controls at indicated times. Results from triplicate measurements are expressed as mean \pm standard deviation bars. (b) *In situ* immunodetection of cleaved caspase-7 in MCF-7 cells treated with azurin. Cells treated with PBS for 24 h did not show cleaved caspase-7 staining (control); however, a significant level of cleaved caspase-7 staining (fluorescing green) could be observed in cells treated with azurin after 12 and 24 h. Nuclei were stained blue with DAPI. Arrows mark the apoptotic cells. Inset to the figure shows a representative cell showing redistribution of cleaved caspase-7 after 24 h of treatment with azurin. (c) Azurin-induced caspase-9 activation in MCF-7 cells. Extracts from MCF-7 cells treated with azurin for various time intervals as indicated were assayed for activation of caspase-9 by Western blot. The amount of processed caspase increases with the time of azurin treatment. β -Actin was used as an internal control. (d) Comet assay showing azurin-induced DNA breaks. In untreated MCF-7 cells, a small amount of inherent endogenous DNA damage could be seen. (e) In contrast, samples treated with azurin show a significant increase in DNA damage, which can be reversed by pretreating the cells with caspase-7 inhibitors. The greater the number of DNA breaks, the larger the comet trails

death. MCF-7 cells treated with azurin showed an increase in the ratio of Bax to Bcl2 as compared to untreated control, while this ratio was not altered significantly in MDA-MB-231 and MDA-MB-157 cells (Figure 3b). Such data suggest that Bax may play an important role in apoptotic events in MCF-7 cells treated with azurin. This Bax translocation occurs along with the release of cytochrome *c* from the mitochondria to the cytosol. Thus, we looked at other events associated with azurin-induced apoptosis in MCF-7 cells. Azurin exposure led to the release of cytochrome *c* from the mitochondria in MCF-7 cells (Figure 3c).

Caspase involvement in azurin-induced apoptosis of MCF-7 cells

Since MCF-7 cells lack caspase-3 owing to the functional deletion in the *casp 3* gene (Janicke *et al.*, 1998), we analysed the activation of executor caspase-7 in azurin-treated MCF-7 cells. Significant levels of caspase-7 processing occurred 8–24 h after treatment with azurin, while there was little such activity in untreated cells (Figure 4a). These results were confirmed by *in situ* caspase-7 processing in azurin-treated MCF-7 cells (Figure 4b). By 24 h, some active caspase-7 staining was even observed in the nucleus, suggesting that

caspase-7 is redistributed as the apoptotic events progress.

Chemotherapy-induced apoptosis by the mitochondrial pathway typically involves caspase-9 activation. Caspase-9 activation was determined by Western blotting. As shown in Figure 4c, treatment of MCF-7 cells with azurin leads to cleavage of procaspase-9 to active caspase-9 within 8 h after treatment, and this increased substantially by 24 h after treatment (Figure 4b, inset).

The effect of azurin treatment on nuclear DNA damage was investigated by quantitative single-cell gel electrophoresis assay (comet assay). MCF-7 cells treated with azurin (50 μ M) for 24 h showed a significant increase in DNA damage (exhibited by many comets) compared to the inherent DNA damage found in untreated cells. These DNA breaks could be reversed to a significant level by pretreatment of MCF-7 cells with 100 μ M caspase-7 inhibitor (Z-DEVD-FMK, Calbiochem, La Jolla, CA, USA) (Figure 4d). The DNA damage in azurin-treated cells was significantly different ($F = 763.67$, $P \leq 0.0001$) from that in untreated cells or cells treated with azurin in the presence of the caspase-7 inhibitor (Figure 4e). In azurin-treated cells, the DNA breaks were quite extensive, as evidenced by large comet trails (Figure 4d), further supporting the hypothesis that azurin-induced apoptosis involves caspase activation.

Protein–protein interaction of azurin–p53 and its role in nuclear transport

A significant mitochondrial and nuclear accumulation of azurin was observed in MCF-7 cells between 12 and 24 h of azurin treatment (Figure 5a). However, in the p53-negative mutant cell line (MDA-MB-157), Western blotting revealed that the bulk of azurin was retained in the cytosol (Figure 5a), suggesting a possible role of p53 in the nuclear transport of azurin.

A GST pull-down assay was used to see if there is a direct interaction between azurin and p53. We used a GST-fused full-length p53 construct or GST constructs containing various nonoverlapping domains of p53, including the N-terminal, Middle region, and C-terminal domains. The GST-associated proteins were pulled down using glutathione sepharose beads, subjected to SDS–PAGE analysis, and then immunoblotted with antiazurin antibody. GST-p53 or the constructs with truncated p53 versions (but not GST or azurin alone) showed coelution of azurin, demonstrating a direct interaction between p53 and azurin. Moreover, azurin was shown to bind preferentially to the N-terminal and Central domain of p53 but weakly to the C-terminal of p53 (Figure 5b). The results of these *in vitro* studies suggest that p53 forms a complex with azurin and perhaps helps in transporting it to the nucleus while azurin, in turn, stabilizes p53. Further studies are in progress to understand the mechanism of regulation of p53 stability by azurin in both cell and cell-free systems. To determine if azurin's complex formation with p53, which has a nuclear import/export signal, allows trafficking of azurin to the nucleus, we microinjected Alexa fluor 568 (fluorescing red) azurin to the cytosol of

both MCF-7 (p53 +/+) cells and MDA-MB-157 (p53 –/–) cells. In MCF-7 cells, azurin remained localized mainly in the cytosol after 20 min and was still there 2 h after microinjection. However, by 4 h, azurin appeared in the nucleus, showing oligosomal DNA condensation suggesting the onset of apoptosis (Figure 5c). In contrast, in MDA-MB-157 cells, azurin remained in the cytosol 4 h after microinjection (Figure 5c) and did not enter the nucleus even after 6 h. This suggests that perhaps p53 is important for the transport of azurin to the nucleus. The mechanism of entry of azurin in a cell remains unclear.

Azurin has less apoptotic effect in normal cells

To test whether azurin induced similar cell death in normal cells, we tested two mammary epithelial cell lines (HBL 100 and MCF-10F). After 72 h of incubation with 57 μ M azurin, only 20% of MCF-10F cells and 18% of HBL100 cells were nonviable. Melanocytes from the foreskin incubated with the same dose of azurin after 72 h resulted in only 16% cell death.

Azurin induces regression of cancer growth and induces apoptosis in vivo

In order to understand the role of azurin *in vivo*, we used a nude mouse model with xenotransplanted MCF-7 cells. In athymic mice treated daily with 1 mg of azurin for 28 days, azurin substantially inhibited tumor growth. Univariate analysis of the data showed that the difference in tumor growth rates between azurin-treated animals and control animals was significant (Figure 6a). For instance, 22 days after the start of treatment, the mean tumor volume in treated mice was only 22% of the mean tumor volume for the control mice (i.e. 0.0267 and 0.1240 cm³, respectively, $P = 0.0179$, Kruskal–Wallis test). When the experiment concluded on the 29th day, the mean tumor volume in the azurin-treated group was only 15% of the mean tumor volume of the control group, an 85% reduction in tumor volume. This is further illustrated by the graph of the mean tumor volumes expressed in cm³ for the two groups over time (Figure 6b). In the multivariate approach, nonlinear mixed-effects models were fitted to the data. The model for tumor growth over time was taken to be exponential with coefficients that were subject-specific mixed effects. For the control group, the fitted model was: tumor volume = $\exp\{-4.23 + 0.06 \cdot \text{time}\}$, while for the treated group it was: tumor volume = $\exp\{-4.23 + 0.03 \cdot \text{time}\}$. The difference was statistically significant ($P = 0.0456$). Taken together, these *in vivo* data suggest that when azurin is administered systemically, it exerts a significant inhibitory influence on the growth and progression of MCF-7 tumor xenotransplants.

During 28 days of treatment, the treated animals did not show any sign of toxicity such as weight loss or other commonly observed signs of toxicity. Furthermore, following necropsy, all viscera were histologically examined, and no discernable alterations were noted

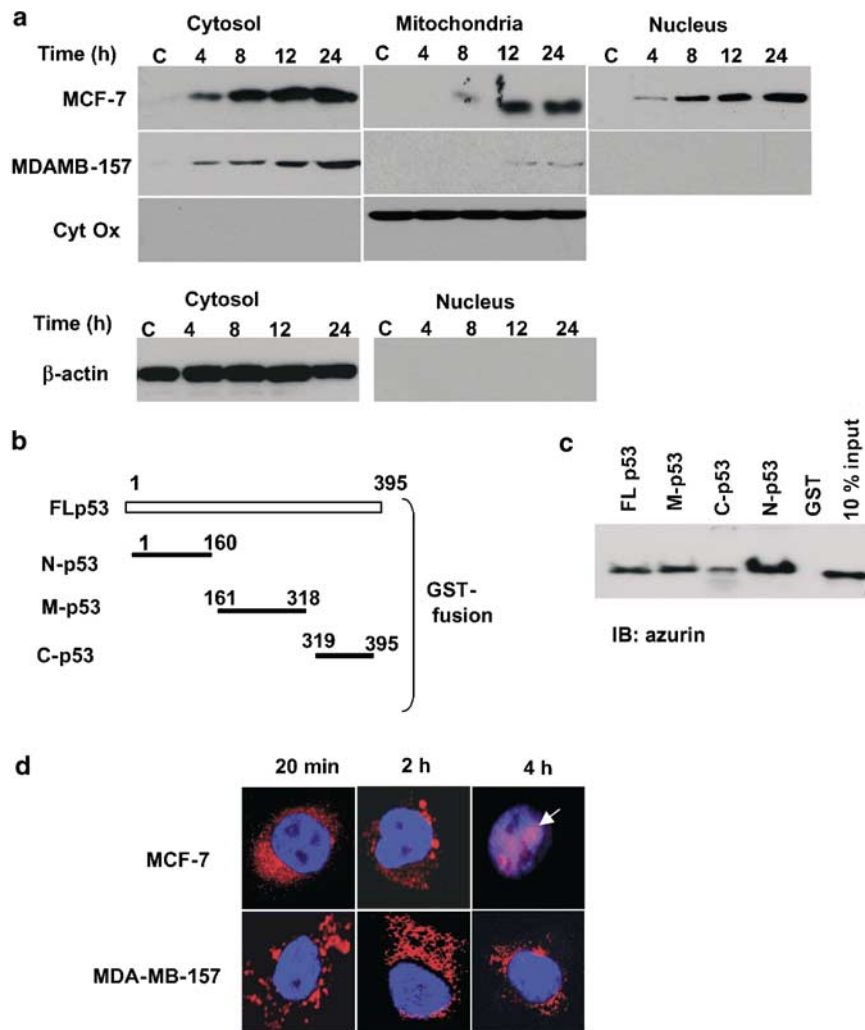


Figure 5 (a) The subcellular localization of azurin in MCF-7 and MD-MB-157 cells. Accumulation of azurin occurs in the nucleus with the time of treatment of MCF-7 cells but not in MDA-MB-157 cells. A portion of azurin also accumulates in mitochondria of MCF-7 cells. In MDA-MB-157 cells, most of the azurin remains in the cytosol. β -Actin and cytochrome *c* oxidase were used as internal controls and for checking cross-contamination of fractions. (b) Genetic constructs used for expression of full length (FLp53), N-terminal (N-p53), Middle region (M-p53), and C-terminal (C-p53). These GST-fused proteins were hyperexpressed in *E. coli*, purified and used for GST pull-down assay. (c) GST pull-down assay to demonstrate complex formation between azurin and full-length p53, N, and M terminal of p53 but only weak binding with C-terminal of p53. IB: Immunoblotting with azurin. (d) Representative confocal microscopic images for subcellular localization of azurin after microinjection of Alexa Fluor 568 labeled azurin (fluorescing red) to MCF-7 cells and MDA-MB-157 cells. After injection, cells were incubated for the indicated times. Nuclei were stained blue with DAPI. Only overlay images are shown

when comparing the viscera of azurin-treated animals to those of controls.

Both control and azurin-treated tumors were morphologically examined. In a routine H&E stain, control tumor parenchyma was intact, with large numbers of dividing cells with mitotic figures (Figure 7a), suggesting an aggressive phenotype. In azurin-treated animals, tumor parenchyma was characterized by scattered areas of disintegration and increased intercellular spaces associated with a remarkable lack of mitotic figures (Figure 7b). The rate of tumor cell proliferation between the control and azurin-treated animals was estimated by Ki-67 antibody staining. In the control group, the tumors showed numerous proliferating cells (Figure 7c), whereas in the azurin-treated group a sharp reduction

was seen in the number of proliferating cells (Figure 7d). The extent of apoptosis in tumors, as estimated by TUNEL stain, showed a marked increase in apoptotic figures in the azurin-treated group (Figure 7f) rather than in the controls, where apoptotic cells were rarely encountered (Figures 7e).

For caspase expression *in vivo*, we relied mostly on immunohistochemistry (Cowan *et al.*, 2001) in our xenotransplant experiments. We first confirmed by TUNEL assay that the regression of tumors was due to apoptosis. In such azurin-treated tumors, we observed a higher level of caspase-9 staining as compared to control tumors (data not shown). In control tumors, caspase-7 was expressed in a few cells (Figure 7g). However, in azurin-treated animals the expression of

a Kruskal Wallis test p-value for significance of azurin treatment

Days	2	4	8	11	14	16	22	25	29
n for control	9	9	9	9	9	9	9	5	5
n for treatment	10	10	10	10	10	10	10	5	5
p-value	.058	.036	.029	.039	.017	.054	.018	.046	.046

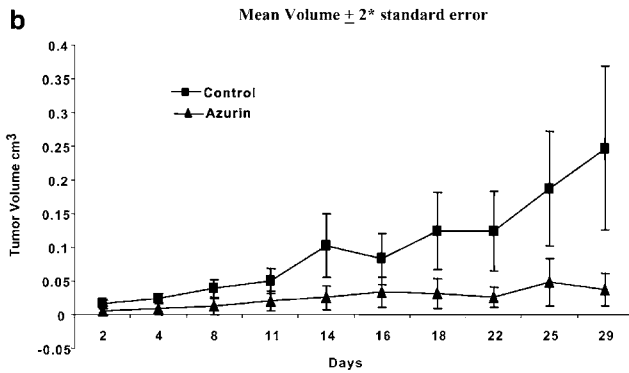


Figure 6 (a) Statistical significance of regression of tumor volume and corresponding *P*-values in response to azurin treatment over untreated control mice in Figure 6b. (b) Regression of MCF-7 xenografts in athymic mice as a function of azurin treatment with time (animals were treated with 1 mg of azurin in 1 ml of normal saline, i.p. daily for 28 days), as compared to the untreated control animals. Bars represent + 2 standard error

caspase-7 was more pronounced in both the nuclei and cytoplasm (Figure 7h, inset). The TUNEL staining and increased expression of caspases indicates that azurin-treated tumors have undergone apoptosis.

Discussion

Several contemporary reports have shown that microbial pathogens replicate at tumor sites under hypoxic conditions and stimulate the host immune response, leading to the inhibition of tumor growth (Alexandroff *et al.*, 1999; Jain and Forbes, 2001; Chakrabarty, 2003). In addition to bacterial pathogens, other infectious agents such as *Toxoplasma gondii* or *Besnoitia jellisoni* are known to activate macrophages and induce tumor regression, presumably through the elaboration of antiangiogenic agents (Hunter *et al.*, 2001). Unfortunately, the use of live microorganisms is always associated with their infectious characteristics and other side effects. As a result of our pursuit to identify a constituent of a cell or its metabolite that may have anticancer activity and can reduce the side effects associated with microorganisms, we have identified, isolated, and purified a bacterial cupredoxin, azurin, that has the potential of regressing tumor growth *in vitro* and *in vivo* in nude mice.

Azurin is a member of a family of low-molecular-weight, soluble, copper-containing proteins called cupredoxins. While a great deal is known about cupredoxins' electron transfer mechanisms, and X-ray

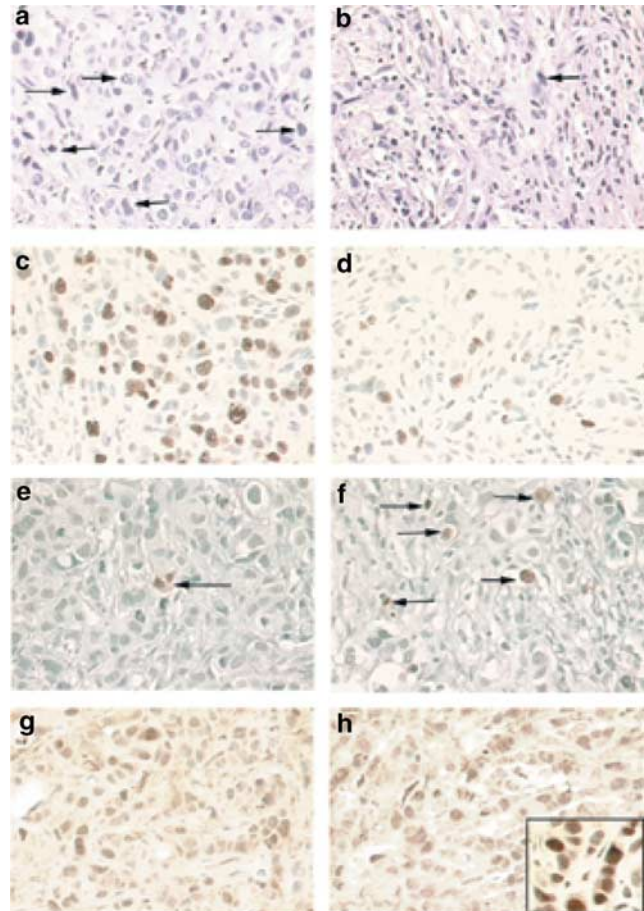


Figure 7 Effect of azurin treatment on morphology, cell proliferation, caspase levels, and apoptosis in MCF-7 xenografted tumors. (a) Untreated control MCF-7 xenotransplant; integrity of the parenchyma is preserved. It is characterized by numerous mitotic figures (arrows) (H&E $\times 40$). (b) Parenchyma of a xenotransplanted tumor from nude mice treated with 1 mg of azurin daily for 28 days. Note the lack of mitotic figures shown by a single arrow ($\times 40$). (c) Control tumor: There is a marked increase in proliferating cells (Ki-67 antibody – brown stain). The slides were counterstained with H&E ($\times 40$). (d) In tumors treated with azurin, there is a sharp reduction in the number of Ki-67 positive (brown-stained nuclei) counterstained with hematoxylin ($\times 40$). (e) Only a few apoptotic cells were observed in control tumors as determined by TUNEL stain (the arrow indicates an apoptotic cell). Counterstained with methylgreen ($\times 40$). (f) A number of apoptotic cells were observed in azurin-treated tumors (shown by arrows). (g) Control tumor with variable levels of caspase-7 expression (brown-stained cells). Expression of caspase-7 is mostly nuclear. Counterstained with hematoxylin ($\times 40$). (h) Caspase-7 expression in treated tumors was increased markedly over untreated controls. In addition to nuclear expression, cytoplasmic staining was frequently observed ($\times 40$). The staining of both nuclei and cytoplasm is better discerned in higher power (inset, $\times 630$). The increase in caspase activity and the TUNEL assay in azurin-treated tumors indicate the apoptotic cascade

crystallographic structures have been solved, very little was known about their cytotoxicity towards mammalian cells until recently, when we reported azurin's ability to trigger apoptotic cell death in sarcoma-transformed cell line-derived J774 macrophages or human melanoma cells (Goto *et al.*, 2003; Yamada *et al.*, 2002a, b). It has

been recently proposed that in response to certain noxious stimuli, both mammalian cells and present day bacteria secrete redox proteins, which in turn induces the cell death. (Punj and Chakrabarty, 2003).

Azurin exerts a high level of cytotoxicity towards MCF-7 cancer cells. The ability of azurin to form a complex with p53—thereby allowing its stabilization (Punj *et al.*, 2003) and consequent high intracellular level in MCF-7 cells—appears to indicate that a p53-dependent mechanism might be the major mode of action of azurin-induced apoptosis in MCF-7 cells. A lack of p53 in MDA-MB-157 cells or the presence of nonfunctional p53 in MDD2 and MDA-MB-231 cells supports this notion since there is a comparative loss of azurin's cytotoxicity towards these cells.

The intriguing question is to what extent azurin-induced apoptosis in MCF-7 cells is based on the intracellular stabilization of p53. p53 is not only able to upregulate transcriptionally particular proapoptotic genes such as *Bax*, *peg3*, *Apaf-1*, *caspase-9*, and *PUMA* but also to repress some antiapoptotic genes like *Bcl-2* (Gross *et al.*, 1998; Budhram-Mahadeo *et al.*, 1999). An increase in the level of p53 can regulate and promote discrete steps of the apoptosis cascade such as upregulation of Bax levels, triggering of Bax translocation to mitochondria, release of cytochrome *c* from mitochondria, activation of apoptosome, etc. We report here that MCF-7 cells containing wild-type p53 were far more sensitive to azurin at all dose levels than were: MDA-MB-157 cells, a p53-negative cell line; MDA-MB-231 cells that contain mutant p53 (codon 280, Arg to Lys) in exon 8 (Runnebaum *et al.*, 1994); or MDD2 cells with a dominant-negative p53. The expression of p53 increased only in MCF-7 cells. Therefore, functional p53 was required for an effective apoptotic pathway in these cells. Bax translocation from the cytosol to mitochondria (Figure 3c) is a classical event in the mitochondrial apoptotic pathway and has been reported to occur in many cell lines in response to various apoptotic stimuli (Gross *et al.*, 1999; Mooney *et al.*, 2002). Bax and Bcl2 play a major role in determining whether cells will undergo apoptosis under experimental conditions. A ratio of Bax to Bcl2—rather than antiapoptotic Bcl2 alone—is important in cell survival or apoptotic death in response to death stimuli (Salomons *et al.*, 1997). The average ratio of Bax:Bcl2 in p53-containing MCF-7 cells treated with azurin was higher than in the untreated control, while in p53-defective cells this ratio remained lower over the untreated control. The low level of cell death in MDA-MB-157 cells could result from the Bcl2-insensitive apoptotic p53-independent pathway (Strasser *et al.*, 2000). Nonetheless, our results showed that functional p53 is important in the p53-dependent pathway leading to apoptosis. However, the possibility of p53-independent cell death in response to azurin treatment might also exist. The results obtained with cells having nonfunctional p53 or no p53 appear to show that the presence of wild-type p53 amplifies the death signal in response to azurin treatment. Furthermore, using GST pull-down assay, we have demonstrated that azurin is capable of directly binding to p53. Apparently,

the protein-protein interaction involved some of the residues beyond the N-terminal: azurin also displayed interaction with the M-terminal. However, there was only a weak interaction between azurin and the C-terminal of p53.

MCF-7 cells are relatively resistant to apoptosis induced by many stimuli because of their loss of functional *casp 3* resulting from the deletion of 47 base pair within exon 3 of the *caspase 3* gene (Janicke *et al.*, 1998). Caspase-7 is related to caspase-3 and shows the same synthetic substrate specificity *in vitro* (Talanian *et al.*, 1997), suggesting that caspase-3 and -7 have possibly overlapping roles in apoptosis (Woo *et al.*, 1998). Caspase-7 can cleave PARP (poly-ADP ribose Polymerase) and DNA fragmentation factor (DFF), which can lead to DNA fragmentation (Enari *et al.*, 1998; Hu *et al.*, 2001; Wojciechowski *et al.*, 2003). It appears that azurin treatment of MCF-7 cells, within 8–24 h, signals the mitochondrial pathway to recruit and activate caspase-9. Caspase-9 then activates caspase-7, which in turn puts into motion a chain reaction that results in apoptotic cell death. Caspase-7 is thought to play the functional role of executor caspase in MCF-7 cells in response to various apoptotic stimuli (Oberhammer *et al.*, 1993; Heerdt *et al.*, 1999; Hishikawa *et al.*, 1999; Zhivotovsky *et al.*, 1999; Liang *et al.*, 2001; Mooney *et al.*, 2002; Lee *et al.*, 2003; Onuki *et al.*, 2003). Moreover, Bax-mediated apoptosis has also been reported to be independent of caspase-3 deficiencies and reconstitution of caspase-3 does not alter overall cell death (Marcelli *et al.*, 1998; Kagawa *et al.*, 2001; Wojciechowski *et al.*, 2003).

Studies using etoposide, doxorubicin, Cisplatin, and key adjuvant drugs for breast cancer treatment concluded that MCF-7 cells were sensitized to apoptosis only when these cells were reconstituted with caspase-3 (Blanc *et al.*, 2000). Our studies have shown that the intrinsic mechanism of apoptosis is functional in MCF-7 cells but is dependent on external stimuli. Azurin can evoke an alternate apoptotic pathway independent of caspase-3, making it a promising agent for combination chemotherapy that merits further study.

Altogether, the most likely sequence of events responsible for azurin-induced apoptosis in MCF-7 cells includes a decrease in Bcl2 level and an increase in the mitochondrial membrane potential with a consequent release of cytochrome *c*. The released cytochrome *c* interacts with Apaf-1, dATP (or ATP), and procaspase-9, leading to the activation of caspase-9, which, in turn, activates caspase-7 and eventually induces apoptosis.

Systemic administration of azurin in MCF-7 xenotransplanted nude mice confirmed azurin's inhibitory effect on breast cancer. Throughout 4 weeks of azurin treatment, there was a dramatic inhibition on tumor growth, and tumor weight had decreased by the end of the experiment. All animals tolerated azurin treatment very well, with no occurrence of any significant differences in body weight between treated and control animals. Based on our results, azurin might prove to be a novel, nontoxic, water-soluble chemotherapeutic agent for human breast cancer. The clinical significance of

these findings—including the efficacy of truncated versions of this redox protein in order to develop a peptide-based anticancer agent (Torchilin and Lukyanov, 2003)—is being investigated.

Materials and methods

Cell lines and reagents

The human breast cancer cell lines MCF-7 (p53+/+), MDA-MB-157 (p53-/-), MDD2 (MCF-7 cell line containing dominant-negative p53), and MDA-MB-231 (mutant p53)—along with the normal breast cells (MCF-10F) and foreskin cells—are all from the stock culture collection of the Department of Surgical Oncology, University of Illinois at Chicago (UIC), Chicago. HBL100 cells were a gift from Dr Nita J Mahile, Department of Biochemistry and Molecular Biology, Mayo Clinic, Rochester, Minnesota.

The cells were grown either in MEM medium supplemented with Earle's salt, 10% FBS and Penicillin/Streptomycin, Macoy's 5A medium, or in RPMI 1640 supplemented with penicillin/streptomycin and FBS. All cells were grown at 37°C in 6% CO₂.

Plasmid constructs

Dr R Baskaran, University of Pittsburgh Medical Center, Pittsburgh, and Dr Thomas Shank, Princeton University, Princeton, kindly provided the various p53-GST constructs used in the present study.

Preparation of azurin

The azurin-encoding gene of *P. aeruginosa* was amplified and cloned in pUC19. Azurin was purified from *E. coli* JM109 as described previously (Yamada *et al.*, 2002a).

Cell proliferation assay

Cell proliferation was analysed by Cell Titer 96 AQueous One Solution Cell Proliferation Assay Kit (Promega, Madison, WI, USA) following the manufacturer's instructions, and as detailed elsewhere (Eilon *et al.*, 2000). Data were calculated as a percentage of untreated control cells.

Annexin-V-FITC assay

Cells (10⁵) were treated with azurin for 4, 8, 12, and 24 h. Detached and adherent cells were pooled, washed with PBS, and resuspended in binding buffer (BD Biosciences). Cells were then stained with annexin-V-FITC antibody as recommended by the manufacturer. Propidium iodide (PI) (final concentration 1 µg/ml) was added immediately prior to analysis by Flow Cytometry. Bivariate analysis of FITC fluorescence and PI fluorescence gave different cell populations, where FITC(-) and PI(-) were designated as viable cells, FITC(+) and PI(-) as apoptotic cells, and FITC(+) and PI(+) as late apoptotic or necrotic cells.

Protein extraction and Western blot analysis

The breast cancer cells were plated and cultured in a complete medium and treated with azurin (53 µM) for various time intervals. The cells were then washed and detached with trypsin-EDTA. Cells were collected by centrifugation and disrupted in lysis buffer (25 mM Tris-HCl (pH 8), 150 mM NaCl, 1% NP-40, 1% sodium deoxycholate, 0.1% SDS,

100 µM DTT, and supplemented with protease cocktail inhibitor) for 30 min (Asher *et al.*, 2001). Cytosolic and mitochondrial fractions were prepared as described by Deveraux *et al.* (1999). The nuclear extracts were separated following the procedure of Raffo *et al.* (2000). For detection of caspase-7 and 9, the treated cells were lysed in lysis buffer containing 20 mM sodium phosphate (pH 7.4), 150 mM NaCl, 0.1% Triton X-100, and 10% glycerol supplemented with a protease inhibitor cocktail tablet. The caspase-9 antibody used here recognizes both cleaved and full-length caspase-9.

Protein contents were determined using modified BioRad Dc assay reagent. In total, 40–60 µg of protein was separated on SDS-PAGE and electrophoretically transferred onto a nitrocellulose membrane. Membranes were then blocked with 1% Western blocking reagent (Roche Biochemicals, Mannheim, Germany) and probed with primary antibody followed by washing in TBS-T (Tris buffered saline with Tween 20). Washed membranes were then probed with the corresponding secondary antibody. After washing, the membranes were treated with enhanced chemiluminescence reagents (Amersham Pharmacia, Piscataway). The specific protein bands were visualized by autoradiography. β-Actin was used as a loading control. The various antibodies used in immunoblotting include p53 polyclonal antibody (Santa Cruz Biotechnology, Santa Cruz, CA, USA), Bax, Bcl2, cytochrome *c* (BD Biosciences, San Jose, CA, USA), caspase-7 and caspase-9 (Cell Signaling, Beverly, MA, USA), Cytochrome *c* oxidase (Molecular Probes, Eugene, OR, USA), and β-actin (Sigma chemicals, St Louis).

Densitometry analysis

Western blots were scanned and analysed using Image Quant version 1.2 software on a Macintosh computer. The bidimensional optical densities were quantified and the relative ratio of the various proteins was calculated.

GST pull down assay

GST-FLp53 (GST fused full-length p53) and the various truncated versions of p53, GST-N-p53 (GST fused N-terminal domain of p53), GST-M-p53 (GST fused Central domain of p53), and GST-C-p53 (GST fused C-terminal domain of p53) were prepared after induction with IPTG and purified using a standard protocol as recommended by the manufacturer (Amersham Pharmacia Biotechnology, Piscataway). Equal amounts of GST-tagged p53 or GST alone and azurin were mixed, and the putative complex was pulled down using Glutathione Sepharose 4B beads. The beads were washed with excess of PBS to remove unbound proteins. As controls, GST, GST-p53, and azurin alone were individually treated using the same procedure as above. Proteins were then subjected to SDS-PAGE and transferred onto a PVDF membrane (0.2 µm, BioRad, Hercules), which was probed with anti-azurin and p53/GST antibodies.

Enzyme-linked immunosorbent assay for caspase-7

An ELISA was standardized to detect specifically *in vitro* endogenous levels of active caspase-7 in the azurin-treated MCF-7 cells over various time intervals using the Quantikine human active caspase-7 immunoassay kit (R&D system, Minneapolis, MN, USA). This procedure specifically detects the cleaved caspase-7, and does not crossreact with procaspase-7. The amount of caspase-7 was calculated from a standard curve, and the results are presented as relative amounts of active caspase-7 as described by Saunders *et al.* (2000). An *in situ* immunodetection of active caspase-7 was

carried out using confocal laser microscopy. In order to study intracellular localization of caspase-7, the procedure of Meller *et al.* (2002) was used with some modifications. Briefly, cells were grown in 0.17 mm delta T dishes (Biopotech, Butler, PA, USA) and treated with azurin for various time intervals as indicated. The cells were washed with PBS and fixed with 3% paraformaldehyde. The fixed cells were permeabilized with 0.1% Triton X-100 in PBS for 15 min. Nonspecific binding sites were blocked with 5% donkey serum (Jackson Immuno Research, West Grove, PA, USA) for 1 h followed by overnight incubation with the primary antibody (cleaved caspase-7; Asp198 antibody; Cell Signaling) in 0.1% BSA in PBS. Cells were washed with PBS before incubating with Cy2-conjugated donkey anti-rabbit IgG secondary antibody for 1 h. After washing the cells with PBS, the nucleus was stained blue with DAPI. Finally, the cells were covered with a thin film of Prolong Antifade reagent (Molecular Probes, Eugene, OR, USA), and images were taken under a confocal microscope. The presence of active caspase-7 is indicated by green fluorescence because of Cy2-conjugated secondary antibody.

Microinjection of azurin in MCF-7 and MDA-MB-157 cells

Microinjection was performed following the basic protocol as described by Gajate *et al.* (2000). Briefly, MCF-7 and MDA-MB-157 cells were cultured overnight on 14-mm glass coverslips coated with poly-D-lysine and adhered to a 35-mm tissue culture dish (Mat Tex Corporation, Ashland, MA, USA). Azurin was chemically labeled (red) with Alexa Fluor 568 (Molecular Probes, Eugene, OR, USA) as recommended by the manufacturer. The labeled azurin was microinjected into the cytoplasm of single cells using a computer-controlled microinjector (AIS 2) system. All microinjection experiments were performed using a 0.5 s injection time and 100 hPa pressure with a Zeiss 200 M microscope. Approximately 75–100 cells were injected in each dish. After microinjection, cells were further incubated at 37°C in 6% CO₂ for varying time intervals. Cells were then fixed with 4% paraformaldehyde, nuclear DNA was stained blue with DAPI, and fluorescent images were acquired with a Zeiss LSM 510 confocal laser microscope and analysed with CLSM software.

Comet assay

The single-cell gel electrophoresis was carried out according to the procedure of the manufacturer with minor modifications (Trevigen, Gaithersburg, MD, USA) as described previously (Salti *et al.*, 2000). Slides were dried in 80% ethanol, stained with SYBR Green (Trevigen, Gaithersburg, MD, USA), and viewed under a fluorescent microscope emitting light between 425 and 500 nm. The cells were qualitatively scored from 0 to 4 according to the size of the comet tail. Cells with a score of zero had intact DNA and cells with a score of four were significantly damaged. The cells were scored according to the equation:

$$\sum (0 * n_0 + 1 * n_1 + 2 * n_2 + 3 * n_3 + 4 * n_4) / N \times 100$$

where n_0 is the number of cells with a score of 0, n_1 is the number of cells with a score of 1, etc., and N is the total number of cells counted. Duplicate samples were prepared for each treatment, and 400 cells were scored for each sample.

In vivo xenotransplant studies

MCF-7 cells (5×10^5) were injected into the lowest right mammary fat pad of estradiol-pretreated female nude mice.

The mice were randomly split into two groups of 10 mice each. The treated group received 1 mg of azurin in 1 ml of normal saline intraperitoneally daily for 28 days, and the control group received 1 ml of saline i.p. daily for 28 days. The treatment started three days after MCF-7 inoculation. On the 29th day, all of the animals were killed and a detailed necropsy was performed. All of the tumors and viscera were preserved for histological and immunocytochemical examination. During the course of the experiment, the mice were examined daily, and 3-axis tumor volume and body weights were measured twice weekly.

Immunohistological methods

Cell proliferation in tumors was evaluated by Ki-67 antibody (U0028, Epos, Dako Co., Denmark). Slides were deparaffinized, heated in a microwave oven for 15 min in citric buffer (0.01%), and covered with antibody for 1 h. The antibody is HPR-conjugated; therefore, after $2 \times$ PBS wash, the slides were stained with DBA and counterstained with hematoxylin for characterization of tumor morphology. Apoptotic cells were evaluated by the TUNEL assay as recommended by the ApopTag *in situ* hybridization detection kit (Oncor, Gaithersburg, MD, USA). The top section on each slide, which was incubated without digoxigenin-dUTP, was used as a negative control. Tissue sections were counterstained with methyl green for visualization of tumor morphology. The expression of caspase-7 was examined by immunohistochemistry on formalin-fixed, paraffin-embedded tumor samples. Tissue sections were treated with a retrieval solution (citric buffer, 0.01%) to increase the intensity of the reaction product. Polyclonal rabbit antibodies from NeoMarker (Fremont, CA, USA) were used at concentrations of 1:200, 1:100, 1:100, and 1:200, respectively. The slides were covered with the corresponding antibody overnight. The ABC kit and DBA staining were employed for the amplification of the signal and the visualization of the antigen. The top section of each slide was used as a control and was not treated with the corresponding antibody. The slides were counterstained with hematoxylin.

Statistical methods

Both univariate and multivariate methods were used. The univariate method consisted of computing the summary statistics for the tumor volume for each group (treated with azurin and control) for each of the 10 days on which measurements were taken. The nonparametric Kruskal–Wallis test was used to examine the differences between the groups at each time point, and P -values were computed to determine the significance of the treatment.

In the multivariate approach, analysis was based on 19 animals (10 treated mice and nine control mice). Exponential models were fitted to the data in order to study the growth of the tumor over time, measured as days from the injection of cancer cells. Analysis was carried out by SAS[®]. For IC₅₀ determination from cell proliferation assay, nonlinear regression analysis was performed with Microsoft Excel to generate curves for the calculation of IC₅₀ (He *et al.*, 2003).

Acknowledgements

We thank Mr Albert Green for helping with the animal studies, Ms Laura Bratescu for maintaining all the cell cultures, and Ms Anne Shilkaitis for helping with immunocytochemical staining of the tumors. Thanks are also due to Drs Thomas Shenk and R Baskaran for genetic constructs, and to Drs N Mahile and CJ Froelich for the cell lines used in this

work. The editorial help and supervision of Mr Scott Kennedy in manuscript preparation is acknowledged. This research was supported by US National Institutes of Health Grants: PHS

ES04050-17, CA09432, CA96517, CA95712, DOD Grant DAMD17-99-1-9223, NSF Grant DMS-0204532, and a gift from the Raymond Cole Foundation.

References

- Alexandroff AB, Jackson AM, O'Donnell MA and James K. (1999). *Lancet*, **353**, 1689–1694.
- Altmann KH, Wartmann M and O'Reilly T. (2000). *Biochim. Biophys. Acta*, **1470**, 78–91.
- Asher G, Lotem J, Cohen B, Sachs L and Shaul Y. (2001). *Proc. Natl. Acad. Sci. USA*, **98**, 1188–1193.
- Bange J, Zwick E and Ullrich A. (2001). *Nat. Med.*, **7**, 548–552.
- Blanc C, Deveraux QL, Krajewski S, Janicke RU, Porter AG, Reed JC, Jaggi R and Marti A. (2000). *Cancer Res.*, **60**, 4386–4390.
- Budhram-Mahadeo V, Morris PJ, Smith MD, Midgley CA, Boxer LM and Latchman DS. (1999). *J. Biol. Chem.*, **274**, 15237–15244.
- Chakrabarty AM. (2003). *J. Bacteriol.*, **185**, 2683–2686.
- Chandler JM, Cohen GM and MacFarlane M. (1998). *J. Biol. Chem.*, **273**, 10815–10818.
- Chou TC, Zhang X, Harris CR, Kuduk SD, Balog A, Savin KA, Bertino JR and Danishefsky SJ. (1998). *Proc. Natl. Acad. Sci. USA*, **95**, 9642–9647.
- Coley WB. (1911). *Surg. Gynec. Obstet.*, **613**, 174–190.
- Cowan CM, Thai J, Krajewski S, Reed JC, Nicholson DW, Kaufmann SH and Roskams AJ. (2001). *J. Neurosci.*, **21**, 7099–7109.
- Cuvillier O, Nava VE, Murthy SK, Edsall LC, Levade T, Milstien S and Spiegel S. (2001). *Cell Death Differ.*, **8**, 162–171.
- Dang LH, Bettgowda C, Huso DL, Kinzler KW and Vogelstein B. (2001). *Proc. Natl. Acad. Sci. USA*, **98**, 15155–15160.
- Deveraux QL, Leo E, Stennicke HR, Welsh K, Salvesen GS and Reed JC. (1999). *EMBO J.*, **18**, 5242–5251.
- Eilon GF, Gu J, Slater LM, Hara K and Jacobs JW. (2000). *Cancer Chemother. Pharmacol.*, **45**, 183–191.
- Enari M, Sakahira H, Yokoyama H, Okawa H, Iwamitsu A and Nagata S. (1998). *Nature*, **391**, 43–50.
- Gajate C, Fonteriz RI, Cabaner C, Alvarez-Noves G, Alvarez-Rodriguez Y, Modolell M and Mollinedo F. (2000). *Int. J. Cancer*, **85**, 674–682.
- Goto M, Yamada T, Kimbara K, Horner J, Newcomb M, Das Gupta TK and Chakrabarty AM. (2003). *Mol. Microbiol.*, **47**, 549–559.
- Gross A, Jockel J, Wei MC and Korsmeyer SJ. (1998). *EMBO J.*, **17**, 3878–3885.
- Gross A, McDonnell J and Korsmeyer SJ. (1999). *Genes Dev.*, **13**, 1899–1911.
- He Z, Ma WY, Hashimoto T, Bode AM, Yang CS and Dong Z. (2003). *Cancer Res.*, **63**, 4396–4401.
- Heerdt BG, Houston MA, Anthony GM and Augenlicht LH. (1999). *Cancer Res.*, **59**, 1584–1591.
- Hishikawa K, Oemar BS, Tanner FC, Nakaki T, Luscher TF and Fujii T. (1999). *J. Biol. Chem.*, **274**, 37461–37466.
- Hu CC, Tang CH and Wang JJ. (2001). *FEBS Lett.*, **503**, 65–68.
- Hu H, Ahn NS, Yang X, Lee YS and Kang KS. (2002). *Int. J. Cancer*, **102**, 250–253.
- Hunter CA, Yu D, Gee M, Ngo CV, Sevignani C, Goldschmidt M, Golovkina TV, Evans S, Lee WF and Thomas-Tikhonenko A. (2001). *J. Immunol.*, **166**, 5878–5881.
- Jain RK and Forbes NS. (2001). *Proc. Natl. Acad. Sci. USA*, **98**, 14748–14750.
- Janicke RU, Ng P, Sprengart ML and Porter AG. (1998). *J. Biol. Chem.*, **273**, 15540–15545.
- Jemal A, Thomas A, Murray T and Thun M. (2002). *CA Cancer J. Clin.*, **52**, 23–47.
- Kagawa S, Gu J, Honda T, McDonnell TJ, Swisher SG, Roth JA and Fang B. (2001). *Clin. Cancer Res.*, **7**, 1474–1480.
- Lamoureaux G, Turcotte R and Portelance Z. (1976). *BCG in Cancer Immunotherapy*. Grune and Stratton: New York.
- Le XF, Marcelli M, McWatters A, Nan B, Mills GB, O'Brian CA and Bast Jr RC. (2001). *Oncogene*, **20**, 8258–8269.
- Lee ATC, Azimathol HCP and Tan AN. (2003). *Cancer Cell Int.*, **43**, 1–8.
- Liang Y, Yan C and Schor NF. (2001). *Oncogene*, **20**, 6570–6578.
- Marcelli M, Cunningham GR, Haidacher SJ, Padayatty SJ, Sturgis L, Kagan C and Denner L. (1998). *Cancer Res.*, **58**, 76–83.
- Marchenko ND, Zaika A and Moll UM. (2000). *J. Biol. Chem.*, **275**, 16202–16212.
- McGee MM, Hyland E, Campiani G, Ramunno A, Nacci V and Zisterer DM. (2002). *FEBS Lett.*, **515**, 66–70.
- Meller R, Skradski SL, Simon RP and Henshall DC. (2002). *Neurosci. Lett.*, **324**, 33–36.
- Mihara M, Erster S, Zaika A, Petrenko O, Chittenden T, Pancoska P and Moll UM. (2003). *Mol. Cell.*, **11**, 577–590.
- Mooney LM, Al-Sakkaf KA, Brown BL and Dobson PR. (2002). *Br. J. Cancer*, **7**, 909–917.
- Oberhammer F, Wilson JW, Dive C, Morris ID, Hickman JA, Wakeling AE, Walker PR and Sikorska M. (1993). *EMBO J.*, **12**, 3679–3684.
- Onuki R, Kawasaki H, Baba T and Taira K. (2003). *Antisense Nucleic Acid Drug Dev.*, **13**, 75–82.
- Paglia P and Guzman CA. (1998). *Cancer Immunol. Immunother.*, **46**, 88–92.
- Pawelek JM, Low KB and Bermudes D. (1997). *Cancer Res.*, **57**, 4537–4544.
- Punj V and Chakrabarty AM. (2003). *Cell Microbiol.*, **5**, 225–231.
- Punj V, Dasgupta TK and Chakrabarty AM. (2003). *Biochem. Biophys. Res. Commun.*, **312**, 109–114.
- Raffo AJ, Kim AL and Fine RL. (2000). *Oncogene*, **19**, 6216–6228.
- Ralph P and Nakoinz I. (1975). *Nature*, **257**, 393–394.
- da Rocha AB, Lopes RM and Schwartzmann G. (2001). *Curr. Opin. Pharmacol.*, **1**, 364–389.
- Runnebaum IB, Yee JK, Kieback DG, Sukumar S and Friedmann T. (1994). *Anticancer Res.*, **14**, 1137–1144.
- Salomons GS, Brady HJ, Verwijs-Janssen M, Van Den Berg JD, Hart AA, Van Den Berg H, Behrendt H and Smets LA. (1997). *Int. J. Cancer*, **71**, 959–965.
- Salti GI, Grewal S, Mehta RR, Das Gupta TK, Boddie Jr AW and Constantinou AI. (2000). *Eur. J. Cancer*, **36**, 796–802.
- Saunders PA, Cooper JA, Roodell MM, Schroeder DA, Borchert CJ, Isaacson AI, Schendel MJ, Godfrey KG, Cahill DR, Walz AM, Loegering RT, Gaylord H, Woyno IJ, Kaluzhny AE, Kryzek RA, Mortari F, Tsang M and Roff CF. (2000). *Anal. Biochem.*, **284**, 114–124.

- Schiffman K, Rinn K and Disis ML. (2002). *Breast Cancer Res. Treat.*, **74**, 17–23.
- Sinha G. (2003). *Nat. Med.*, **9**, 1229.
- Strasser A, O'Connor L and Dixit VM. (2000). *Annu. Rev. Biochem.*, **69**, 217–245.
- Sznol M, Lin SL, Bermudes D, Zheng LM and King I. (2000). *J. Clin. Invest.*, **105**, 1027–1030.
- Talanian RV, Brady KD and Wong WW. (1997). *J. Biol. Chem.*, **272**, 9677–9682.
- Tangri S, Ishioka GY, Glenn Y, Huang X, Sidney J, Southwood S, Fikes J and Sette A. (2001). *J. Exp. Med.*, **194**, 833–846.
- Tong WG, Ding XZ, Witt RC and Adrian TE. (2002). *Mol. Cancer Ther.*, **1**, 929–935.
- Torchilin VP and Lukyanov AN. (2003). *Drug Disc. Today*, **8**, 259–266.
- Woo M, Hakem R, Soengas MS, Duncan GS, Shahinian A, Kagi D, Hakem A, McCurrach M, Khoo W and Kaufman SA. (1998). *Genes Dev.*, **12**, 806–819.
- Wojciechowski J, Horky M, Gueorguieva M and Wesierska-Gadek J. (2003). *Int. J. Cancer*, **106**, 486–495.
- Yamada T, Goto M, Punj V, Zaborina O, Chen ML, Kimbara K, Majumdar D, Cunningham E, Das Gupta TK and Chakrabarty AM. (2002b). *Proc. Natl. Acad. Sci. USA*, **99**, 14098–14103.
- Yamada T, Goto M, Punj V, Zaborina O, Kimbara K, DasGupta TK and Chakrabarty AM. (2002a). *Infect. Immun.*, **70**, 7054–7062.
- Zhivotovsky B, Samali A, Gahm A and Orrenius S. (1999). *Cell Death Differ.*, **6**, 644–651.